Design and realization of a gripper for the SHERPA robotic arm

R. (Rens) Werink

BSc Report

Committee:
Dr. R. Carloni
É. Barrett, MSc
Prof.dr.ir. A. de Boer

July 2016

013RAM2016
Robotics and Mechatronics
EE-Math-CS
University of Twente
P.O. Box 217
7500 AE Enschede
The Netherlands

Contents

Chapter 1

Introduction

The SHERPA project (Smart collaboration between Humans and ground-aErial Robots for imProving rescuing activities in Alpine environments) [6] is a european project aimed at rescue operations in alpine environments. This is done by utilizing different types of drones and ground vehicles and creating a collaboration between these robots and the operator.

As part of this SHERPA project, the team at the University of Twente is developing a robotic arm to be placed on a rover. This arm is used to pick up small-scale Unmanned Aerial Vehicles (UAVs) from the ground and dock them on the rover to recharge the batteries. Part of this arm is the gripper, which has to secure the UAVs to the arm.

The gripper will be designed to grab an interface shaped as a ring with a diameter of 72 mm which is attached to the UAV. It will contain three fingers placed under an angle of 120 deg in a linear guide which will grab the interface from the inside, the placement of the fingers can be seen in the concept in figure 1.1a. These fingers will be moved using a single actuator inside the gripper. The fingers will be based on a quadrilateral shape that surrounds the interface as it closes, as visualized in figure 1.1b. In this report, the fingers and the actuation mechanism of this gripper will be designed and realized.

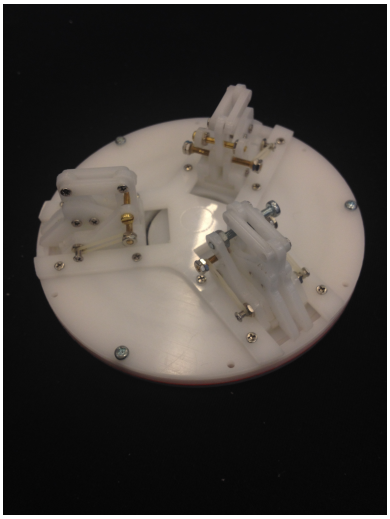

(a) Concept of the gripper showing the positioning of the fingers.

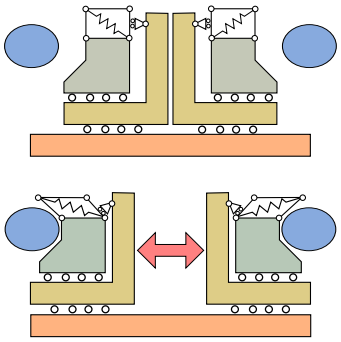

(b) Conceptual drawing of the finger.

Figure 1.1

1.1 Requirements

In this section the requirements for the gripper will be listed.

Dimensions

To limit the size of the gripper, a requirement has been set to keep the diameter and height under 100 mm. As stated previously, the diameter of the interface is 72 mm, this means that the fingers need to travel along the guide, this can be seen in figure 1.1b, where the needed stroke is, depending on the size of the finger, approximately 10 mm

Payload

The gripper should be able to hold the weight of the UAV, which will be approximately 2.5 kg. This weight can in some orientations be acting on a single finger in several directions. The fingers must therefore be able to withstand this weight individually.

Weight

To keep the load on the rest of the arm low, the weight needs to be kept low. This requirement can be fulfilled by using light materials, these however have the downside of being not very strong or they are expensive. The main source of weight will be the motor and gearbox. The gripper should not be heavier than 0.5 kg

Error margin

The downside of the gripper making contact from the inside is that it has to be positioned inside the interface. This requires an error margin within which the gripper can successfully mate with the UAV. The overall shape of the gripper should be such that this margin is maximal, a feasible linear error margin will be about 20 mm.

Closing time

The speed of the gripper should be high to speed up the loading process. The downside of a high gripping speed is the need for a strong motor and strong parts in the gripper, which both add weight and costs. A goal for this requirement is a closing time of less than 0.5 sec.

Actuation

To keep weight and size low, the actuation shall be based on a system with a single motor.

1.2 Comparable gripper

To compare the requirements of the SHERPA gripper to existing designs and to gain inspiration for the design of the SHERPA gripper, an existing gripper design will be presented and compared to the requirements.

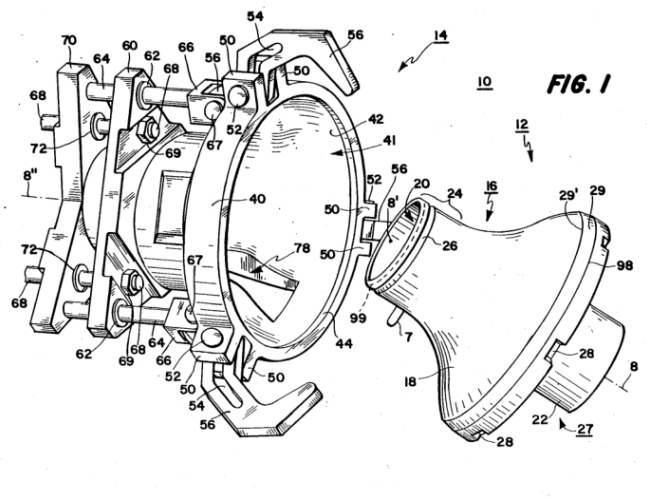

Figure 1.2: A special purpose end effector developed by Matthew Braccio, David W. Gross and John J. Zimmer for the General Electric company [5].

Figure 1.2 features a single interface gripper designed for situations where it is necessary for a robotic arm to change its tool. The inside houses connectors for power and control signals.

This gripper meets some of the requirements of the SHERPA gripper, primarily in the error margin. Due to the shape of the end effector and the interface, the gripper has a lateral margin of about half the size of the gripper. It also has a rotational error margin due to a pin that slots into the gripper.

After closing this gripper rotationally locks the interface to it by inserting its fingers into slots on the interface.

Chapter 2

Design

2.1 Introduction

In the first part of this chapter a finger design will be introduced and an analysis will be performed to find optimal dimensions for the fingers.

In the second part of the chapter, several actuation mechanisms will be compared to find the best for this gripper.

2.2 Fingers

The design of the finger is based on a quadrilateral shape where one of the sides will be parallel to the surface, This is side a in figure 2.1. One end of this side will form the interface point for the ring mounted on the UAV. The motion of this side displacing will be transmitted through the structure with the aid of a pin fixed to the outside world at a fixed height. The resulting motion of the quadrilateral will cause beam d to close down on the ring, this will catch the ring between itself and and an anvil attached to beam a. In this chapter, the influence of the link lengths on the behavior of the fingers and the forces inside will be analyzed.

First, some constants must be defined. These will be first of all the four lengths of the links, which will be called l_a, l_b, l_c and l_d. Then the height of the pin is defined, which is called h_p. The displacement of beam a due to the closing of the finger will be d_a These definitions are also in figure 2.1.

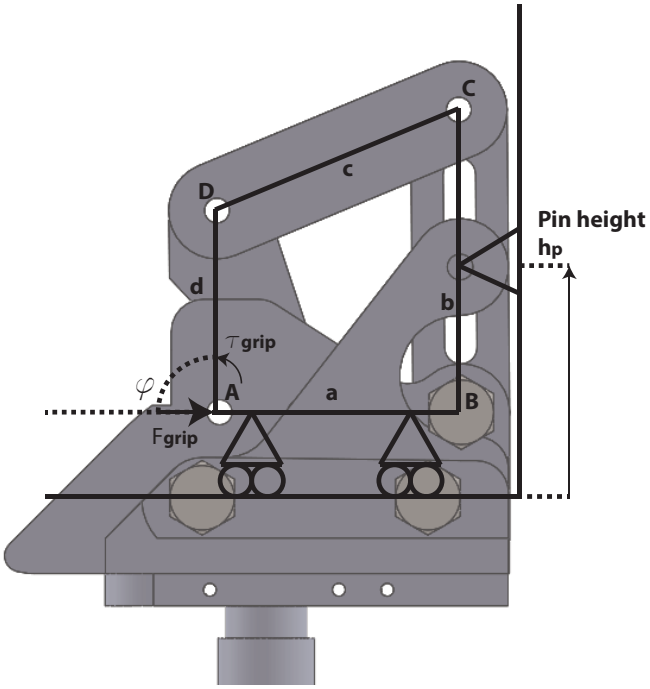

(a) Opened position.

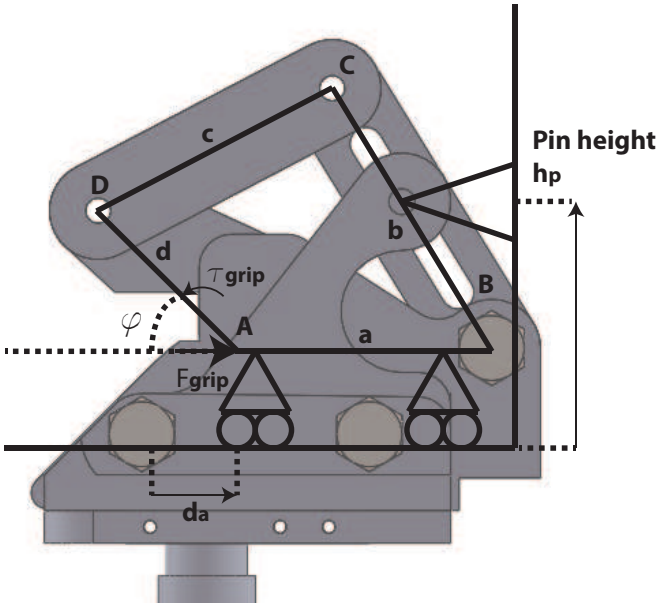

(b) Closed position.

Figure 2.1: Sketches of the definition of the beams and contact points overlaid on a CAD drawing of the finger in the opened and closed position.

From a small angle analysis of the system on the forces in the finger, it can be found that:

$$\tau_{grip} = F_{grip} \cdot \frac{d}{b} \cdot h_p$$

The transmission in force, which is the ratio between the gripping force and the gripping torque is therefore:

$$i_{force} = \frac{\tau_{grip}}{F_{grip}} = \frac{d}{b} \cdot h_p \tag{2.1}$$

A comparable analysis in the movement of the beams yield the following relation for small angles.

$$\varphi = d_a \cdot \frac{b}{d} \cdot \frac{1}{h_p}$$

The transmission in movement, which is the ratio between the displacement of a and the closure angle φ, is therefore:

$$i_{mov} = \frac{\varphi}{d_a} = \frac{b}{d} \cdot \frac{1}{h_p} \tag{2.2}$$

or compared to the force transmission:

$$i_{mov} = \frac{1}{i_{force}} \tag{2.3}$$

From these equations, it can be seen that the transmission of movement is inversely proportional to the transmission of force, which can be expected, as the required work is constant. They are both influenced by the height of the pin(h_p) and the ratio between the lengths of beams b and d.

In the following section, the transmission of movement in the finger will be analyzed by varying the length of beam b and the height of the pin(h_p). This transmission is also relatable to the transmission of force.

Vectors can be defined for the corners of the quadrilateral, which will be called $\overrightarrow{p_A}$, $\overrightarrow{p_B}$, $\overrightarrow{p_C}$ and $\overrightarrow{p_D}$ and the vector $\overrightarrow{p_p}$ for the location of the pin. (0,0) will be defined as the position of $\overrightarrow{p_A}$ in the resting position, i.e. no displacement.

After displacement, the vectors p_A and p_A can be defined:

- $\overrightarrow{p_A} = (d_a, 0)$
- $\overrightarrow{p_B} = (d_a + l_a, 0)$

The pin is located above point B at rest: $\overrightarrow{p_p} = (l_a, h_p)$. Using this vector, the location of point C can be found:

$$\overrightarrow{p_C} = (l_a + d_a \cdot (1 - \frac{l_b}{\sqrt{d_a^2 + h_p^2}}), h_p \cdot \frac{l_b}{\sqrt{d_a^2 + h_p^2}})$$

Now that the positions of points A and C are know and the lengths of beams c and d are constant, the position of point D can be found. This is done by defining circles around A and C with radii l_d and l_c respectively:

$$circle_d : (x - d_a)^2 + y^2 = l_d^2$$

$$circle_c : (x - (l_a + d_a \cdot (1 - \frac{l_b}{\sqrt{d_a^2 + h_p^2}})))^2 + (y - h_p * \frac{l_b}{\sqrt{d_a^2 + h_p^2}})^2 = l_c^2$$

The position of D is located on the intersection of these circles. From the locations of points A and D, the closing angle φ can be found.

The following analyses are performed using chosen values to find the relation between the dimensions in the finger and the influence on the behavior of the finger. With respect to the requirements and the size of the ring, which has a radius of $36mm$, the following values are chosen for the size of the fingers to compare.

- $l_a = l_a = 15\,mm$.
- $l_b = l_d = 12.5\,mm$.
- $h_p = 6\,mm$.
- $d_a = 8.5\,mm$ at full closure.

As stated before, the influence of changes to the finger on the transmission of movement will be analyzed. This will first be done by changing the length of beam b to change the ratio between the lengths of beams b and d. Then the change in pin height will be investigated. A benefit of these changes is that the influence of the remainder of the geometry is minimal.

2.2.1 Pin height

The influence of changing the height of the pin is easy to imagine, if the pin is lowered, the top of beam b will deflect more with the same displacement of beam A. This can also be found from equation 2.2. However, this change is constrained by the fact that it has to fit into beam b, limiting the pin height to a small range of values as to fit into a slot in beam b.

The influence of changing the pin height from the reference design is visible in figure 2.2. The heights used for the comparison of the pin are *a*) $5\,mm$, *b*) the original $6\,mm$ and *c*) $7\,mm$.

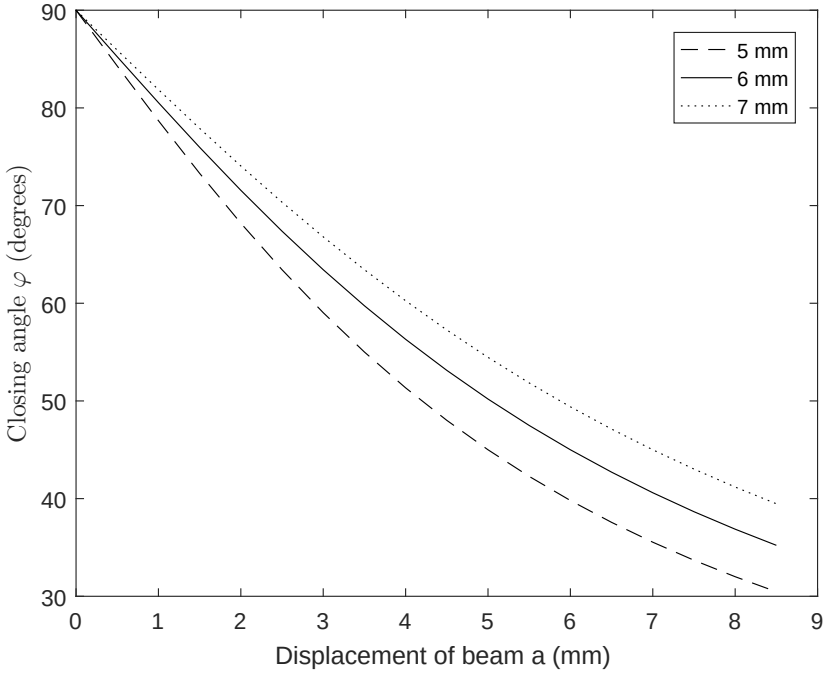

Figure 2.2: Relationship between deflection of beam a and closing angle φ for different pin heights.

As can be concluded from figure 2.2, the slope does indeed change as expected from equation 2.2. Also, due to the limited change in pin height, the resulting change in transmission is also limited to a small range.

2.2.2 Length beam b

The change in the length of beam b will also be investigated, as this will change the $\frac{b}{d}$ component of equation 2.2. In this comparison, the length of beam c will change accordingly to keep beams b and d perpendicular to beam a in the resting position.

Two comparisons will be made, in the first case, the length of beam b will be altered without changing the height of the pin. In the second comparison the pin height will change according to the length change of beam b. These changes should cancel out in equation 2.2. However, as this is a small angle approximation, it will not hold for larger deflections of beam a.

The lengths investigated for beam b are *a*) the original $12.5mm$, *b*) $18.75mm$ and *c*) $25\,mm$. These have been chosen as the are respectively 1.5 and 2 times the original length. This causes the angle of beam c to increase to respectively $14.0°$ and $33.7°$.

When only changing the length of beam b, it can be expected that the

closing angle φ decreases as well. This can be seen in figure 2.3, in which the dotted line is located at 0°, as it is not physically possible to have a closure angle below 0°.

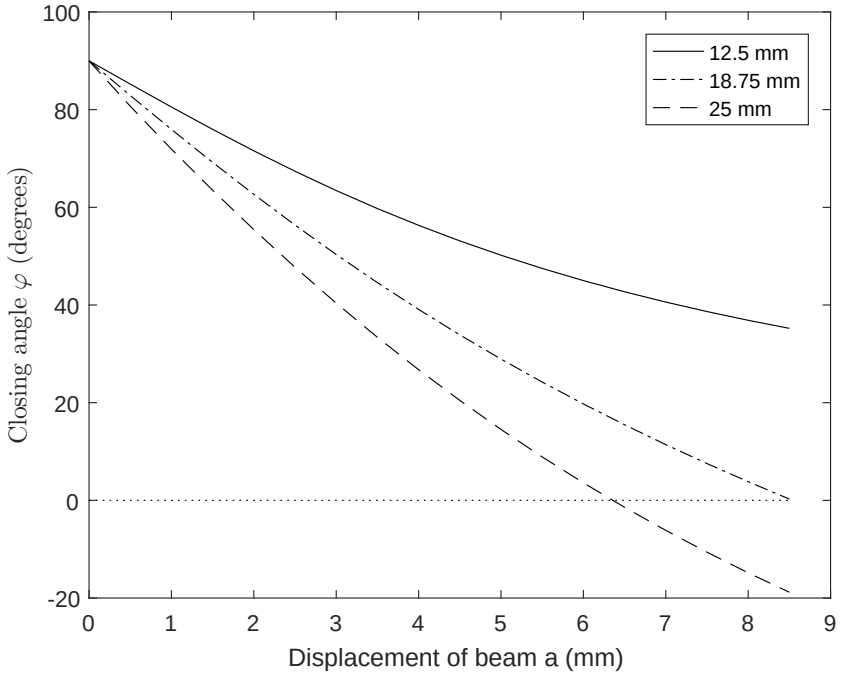

Figure 2.3: Relationship between deflection of beam a and closing angle φ for different lengths of beam b without moving pin.

This agrees again with equation 2.2, increasing the length of beam b does increase the movement transmission.

In an effort to find out the relation between changing beam b and changing the pin height in relatively high displacements, both were changed simultaneously in figure 2.4. The pin height and the length beam b have been changed by the same factor as to keep the small angle transmission equal.

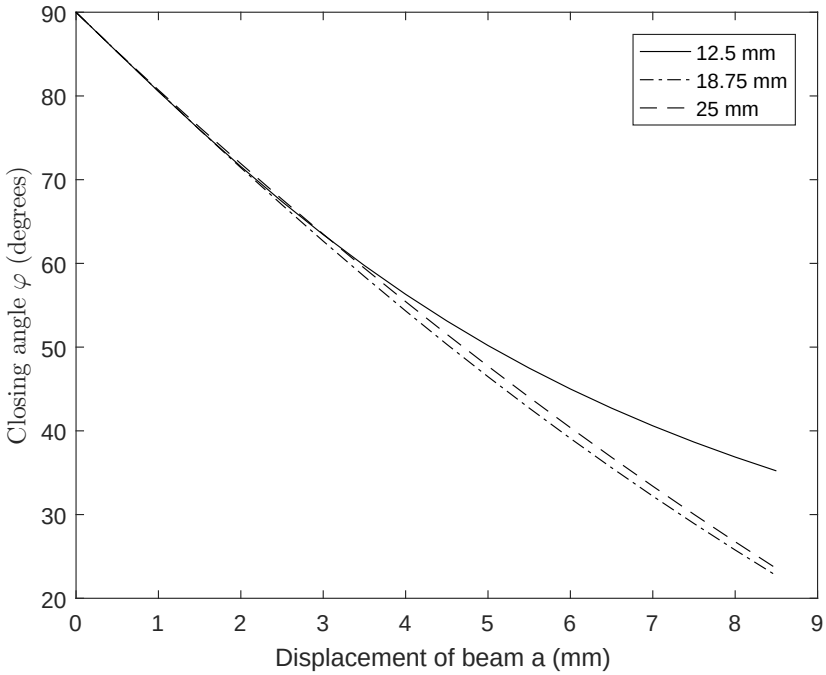

Figure 2.4: Relationship between deflection of beam a and closing angle φ for different lengths of beam b while moving pin.

From this figure, two things can be concluded. Firstly that the transmission is indeed unchanged for small displacements. Secondly, it can be seen that this specific combined change of pin height and beam b has caused the transmission to become more linear for larger displacement.

2.2.3 Conclusion

To prevent the force transmission from increasing, which causes larger stresses in the finger when closed. The final design of the finger will be based around the reference design with beam b lengthened to $18.75mm$ and the pin height changed accordingly. This also creates a point on the top of the gripper, which could help with aiming if no other guides were implemented.

2.3 Actuation Concepts

To move these fingers, which are mounted on a baseplate, an actuation system has to be designed. This system needs to move the fingers in a straight line. As stated in the introduction, they will be based around a single actuator.

In this section, three different actuation concepts are presented and compared according to the following requirements.

The system should, in decreasing order of importance, *a*) be capable of gripping and supporting the UAV as it is picked up, *b*) use the least amount of parts, as to avoid complexity in the design and *c*) be as compact as possible.

2.3.1 Crank

This design consists of two arms per finger which transforms the rotational motion of the motor shaft to the desired linear motion of the finger base.

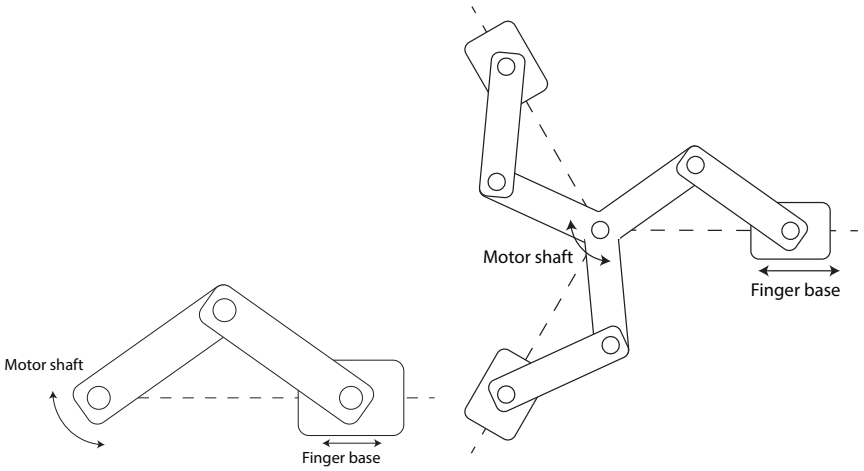

(a) A sketch of the basic function of a crank system.

(b) A sketch of the complete system with three arms and a center assembly.

Figure 2.5

Advantages of this system are that *a*) it only consists of four moving parts in total and *b*) it has the possibility of latching behavior, which means that it can lock itself in place in the extended position.

To elaborate on these advantages; this design will work with only four moving parts, 3 arms attached to the fingers and a center arm assembly attached to the motor as can be seen in figure 2.5b.

The disadvantage of this system is that it is back-drivable, which means that a load applied at the finger will cause the system to move if the motor is not turned on. This problem can be circumvented by moving the motor at or slightly past the singularity position of the arm (which is when the two arms are in a straight line) and adding a fixed endstop at this position such that it 'locks' itself in place against the endstop and secures the fingers. This endstop can be attached to either the housing or one of the arms to not add any moving parts.

2.3.2 Cam

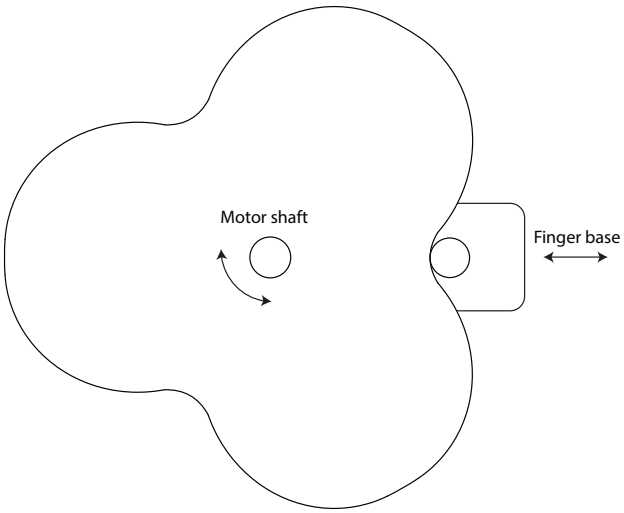

Figure 2.6: Sketch of the basic function of the cam actuation system.

Another implementation is a cam system that rotates inside the assembly, pushing away the fingers from the center of the gripper. The fingers will subsequently be pulled back by a return mechanism. The advantage of this implementation is that is uses a minimal amount of moving parts.

The downside of this implementation is that it uses a large disc that takes up a large part of the space and the necessity of a return mechanism. It is also back-drivable at points where the radius is not constant, this can be solved by introducing a flat part in the cam, i.e. a part where the radius is constant and the induced torque on the motor shaft zero. This will be elaborated later in section 2.5.

2.3.3 Half radius gears

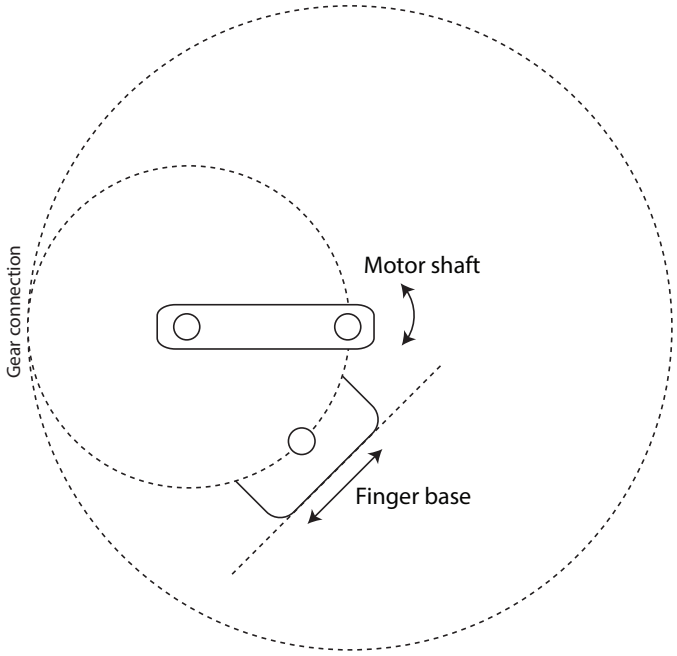

Figure 2.7: Sketch of the half radius gear system. The dashed lines represent the teethed surfaces. It also shows the arm which translates the motion of the motor shaft into the movement of the inner gear.

This design is based on the property that planetary gears inside a gear ring with twice the radius of the planetary gears have points that move in straight lines. This system has the advantage of being quite simple if it consists only of one gear. The disadvantage therefore comes from the fact that it needs to move three fingers, this requires three planetary gears. This means that the gears are hard to fit in the design, they either have to be layered, which takes more space or the gears need a specific design to not interfere with each other, which causes them to be hard to manufacture and expensive. Each gear also needs to be mounted on an arm as they need to move inside the assembly, this adds more moving parts and size to the implementation.

2.4 Comparison of concepts

Based on these concepts, table 2.1 can be made, which summarizes the advantages and disadvantages of each system.

	Complexity	Weight	Compact
Crank	Medium	Light	Yes
Cam	Low	Light	Yes
Half radius gears	High	Medium	No

Table 2.1: Comparison between different methods of actuation.

The crank system has been labeled as medium complexity, due to the 6 joints that need to be connected rigidly. Due to the required additional parts in the implementation of the gears the system becomes more complex, adding to the weight and the size. The final design will be chosen from the crank and cam systems in the following sections.

2.5 Crank

This design consists of 2 beams, a and b, that are hinged together as can be seen in figure 2.5. One end is driven by a motor and the other is free to slide along a linear guide.

For these analyses, a finger stroke from 10 mm to 20 mm will be considered. Three rotations will be considered, two rotations from the singularity position ($\theta_a = 0$) to 45° and 60° to find the relation between different closure angles and a rotation from 30° to 60° to find the behavior when not starting from the singularity position. The lengths of the arms are derived directly from the stroke of the finger and the wanted rotation of the motor shaft using equation 2.4, which describes the position of the finger as a function of motor rotation and beam lengths. The solution to this equation in both the opened and closed positions gives the lengths of the beams.

$$p_{finger} = cos(\theta_a) \cdot a + \sqrt{1 - \frac{a^2 \cdot sin^2(\theta_a)}{b^2}} \cdot b \tag{2.4}$$

It can be expected that a larger rotation of the motor shaft leads to a lower transmission of force as the same work needs to be done to move the finger.

2.5.1 Torque analysis

In this analysis, the needed torque on the motor axle to hold a certain load on the fingers will be derived. In this derivation the load will be denoted as F_{par} and is assumed to be working directly towards the axle of the motor.

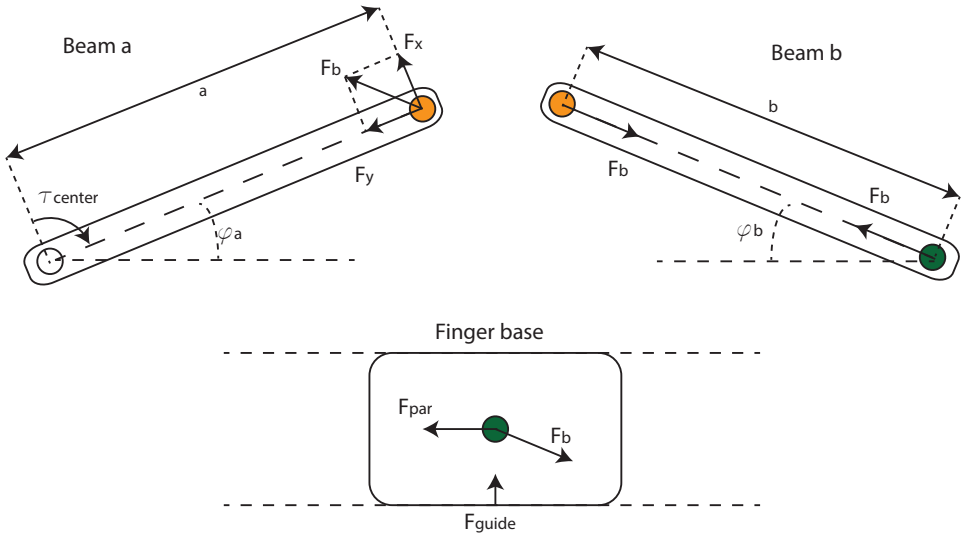

Figure 2.8: Free body diagrams of the three parts that make up a crank system, including the definitions used in the analyses. Equally colored joints are hinged together.

From this, the force in the direction of the second arm (b) is proportional to the cosine of the angle to the force/center line θ_b.

$$F_b(\theta_b) = \frac{F_{par}}{cos(\theta_b)} \tag{2.5}$$

this angle θ_b depends on the lengths of a and b and the angle of a:

$$\theta_b = sin^{-1}(\frac{a \cdot sin(\theta_a)}{b}) \tag{2.6}$$

This normal force is then acting on beam a with an arm of $a \cdot sin(\theta_a + \theta_b)$ to generate a torque on the center axle:

$$\tau_{center}(\theta_a) = F_{par} \cdot \frac{a \cdot sin(\theta_a + sin^{-1}(\frac{a \cdot sin(\theta_a)}{b}))}{\sqrt{1 - \frac{a^2 \cdot sin^2(\theta_a)}{b^2}}} \tag{2.7}$$

The angle-torque relationship is plotted in figure 2.9 for each of the analyzed ranges, this figure is based on a load of 35 N at the finger.

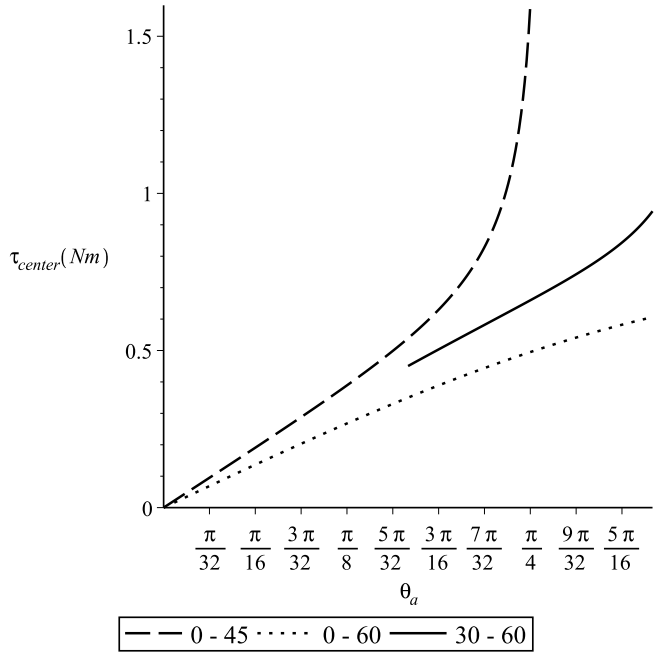

Figure 2.9: The relationship between the angle of beam a and the needed torque at the motor shaft for a load of 35 N for the cases considered in the analysis.

As expected, a larger rotation leads to a lower transmission of torque. It can also be seen no torque is needed to hold the finger when θ_a approaches zero, this is where the singularity position of this system is. The rotation of 30° to 60° follows the general shape of the other cases, but does not start at 0, as can be expected.

2.5.2 Force analysis

The same style of analysis can be used the other way around, to assume a certain amount of torque on the center axis, this torque will be denoted as τ_{center}. The force needed at the finger to hold the system can then be derived. This relation should be inversely proportional to the torque analysis performed earlier.

The force in the direction of rotation at the end of beam a is

$$F_x = \frac{\tau_{center}}{a}. \tag{2.8}$$

This is then transferred to b under an angle of $\theta_a + \theta_b$ so the transferred force is:

$$F_b(\theta_a) = \frac{\tau_{center}}{a \cdot sin(\theta_a + \theta_b)}. \tag{2.9}$$

This force can the be split into the component in the direction of motion of the finger.

$$F_{par}(\theta_a) = \frac{\sqrt{1 - \frac{a^2 \cdot sin^2(\theta_a)}{b^2}}}{a \cdot sin(\theta_a + sin^{-1}(\frac{a \cdot sin(\theta_a)}{b}))} \cdot \tau_{center} \tag{2.10}$$

In the figure (2.10 the force needed parallel to the direction of movement to hold the system is plotted, a torque of 1 Nm is assumed on the center axle for the calculations.

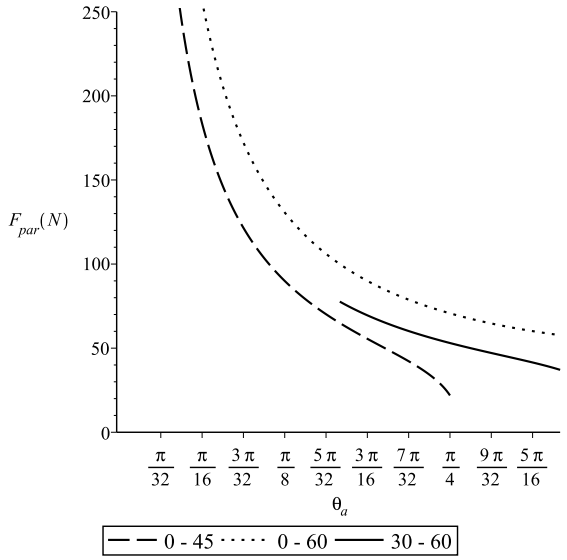

Figure 2.10: The force needed in the direction of motion with an input torque of 1 Nm as a function of the angle of beam a.

The relation between displacement and force at a constant torque is indeed the inverse of the relation between displacement and torque at a constant force.

2.5.3 Conclusion

From the previous figures, it can be seen that indeed when the system approaches the singularity position, the system is very resistant to a load on the finger. This can be very beneficial to an application of this system. As can be expected, a larger rotation of the motor does decrease the needed torque. It is beneficial for the material requirements to keep forces in the system low. It is therefore best to use this system with a large motor displacement starting at the singularity position ($\theta_a = 0$).

2.6 Cam

This design relies on a disc with a changing radius, on which the finger assembly is resting using a bearing as contact point. The design freedom in this design is the displacement angle (which is the angle between fully closed and fully open) and the profile of the cam surface.

The two profiles that will be considered are a linear profile and a sine profile. These profiles describe the radius of the cam as a function of the angle. The stroke of the finger base and therefore the cam surface will be equal to the analysis of the crank, between $10\,mm$ and $20\,mm$. The extreme values in the final design are dependent on the position of the bearing with respect to the gripping point of the finger and the size of the finger.

The linear profile will simply increase linearly with angle between the 2 extreme values. The sine profile will be chosen such that the outer surface follows the shape of a quarter sine, where the closed position is when the sine hits an extreme value. Plots of these profiles can be seen in figure 2.11, where the radius is plotted against an angle around the center of the disc.

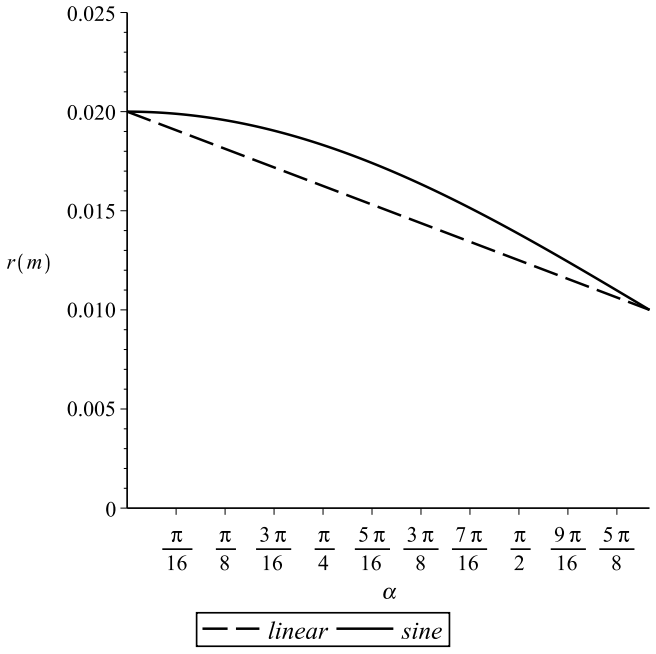

Figure 2.11: The two profiles considered.

To illustrate these profiles further, the actual cams can be seen in figures 2.12a and 2.12b. These are cams that are designed to turn 60° from open to closed.

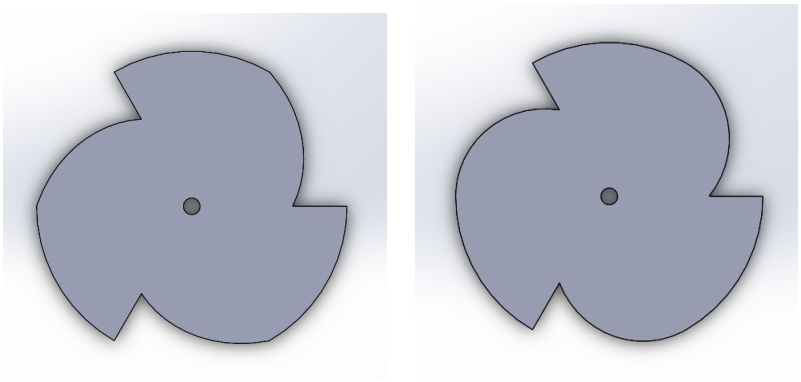

(a) Linear profile *(b) Sine profile*

Figure 2.12: Two different cam profiles.

For this analysis, the following angular displacements are considered for both profiles: *1*) 30°, *2*) 45° and *3*) 60°. These values are chosen to fit 3, 4 or 6 full profiles on a cam.

2.6.1 Torque analysis

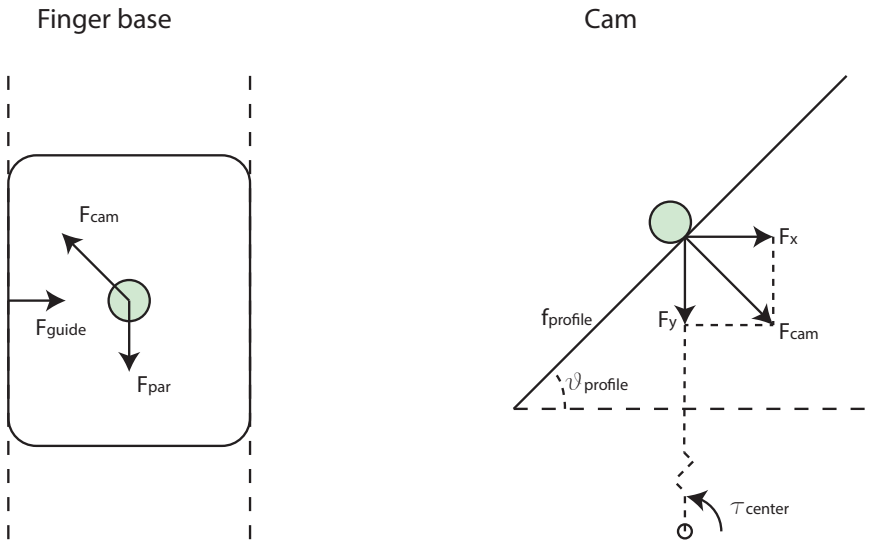

Figure 2.13: Diagram of the definition of forces in the analysis, on the left are the forces working on the finger and on the right the forces on the cam.

As with the crank system, the needed torque to hold a load on the finger can be derived. The forces mentioned can be seen in Figure 2.13. Assuming that the force acts directly towards the center of the disc and has a value of F_{par} acting on the pin, the component of the force that is exerted perpendicular

to the surface of the cam can be found with a force equation on the finger:

$$F_{par} = F_{cam} \cdot cos(\theta_{profile}) \tag{2.11}$$

To calculate this surface angle of the cam($\theta_{profile}$), the slope of the profile is needed, this slope can be found by taking the derivative with respect to the angle of rotation (α):

$$slope(\alpha) = \frac{df_{profile}}{d\alpha} \tag{2.12}$$

As this slope is with respect to the angle, the derivative needs to be multiply by $\frac{1}{r}$ to get the slope with respect to the distance traveled, this slope can then be used to find the contact angle using the inverse tangent.

$$\theta_{profile}(\alpha) = tan^{-1}(\frac{1}{r} \cdot \frac{df_{profile}}{d\alpha}) \tag{2.13}$$

The force acting perpendicular to the profile is then found from equation 2.11:

$$F_{cam}(\alpha) = \frac{F_{par}}{cos(\theta_{profile}(\alpha))} \tag{2.14}$$

This force is creating a radial force F_x around the center:

$$F_x(\alpha) = F_{cam}(\alpha) \cdot sin(\theta_{profile}(\alpha)) \tag{2.15}$$

The $\frac{sin()}{cos()}$ term cancels the inverse tangent in equation 2.13 giving the equation:

$$F_x(\alpha) = F_{par} \cdot \frac{1}{r} \cdot \frac{df_{profile}}{d\alpha} \tag{2.16}$$

the torque induced by this force is therefore:

$$\tau_{center}(\alpha) = f_{profile}(\alpha) \cdot F_{par} \cdot \frac{1}{r} \cdot \frac{df_{profile}}{d\alpha} \tag{2.17}$$

This torque can now be plotted for all angles for all 6 variations, as can be seen in figure 2.14.

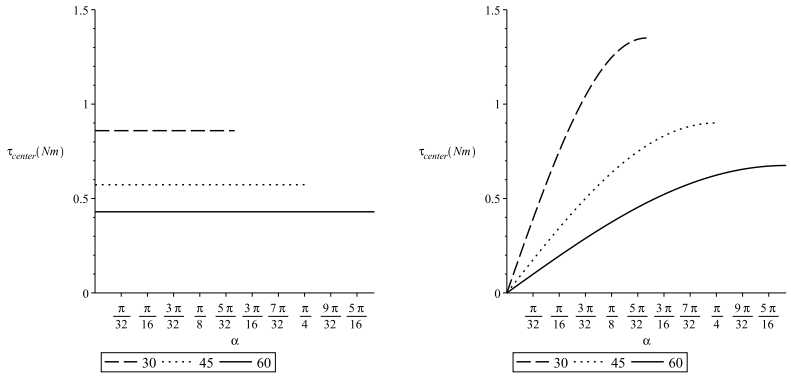

(a) Linear profile *(b) Sine profile*

Figure 2.14: The angle-torque figure for a load of $45\,N$ *applied at the finger.*

From this comparison, it can be seen that the sine profiles have the great advantage that the needed torque approaches zero when the gripper closes. As the torque is not too high, it is feasible to use the sine profiles as the highest load will be applied near the end of the closing sequence. The inverse relation between motor rotation and required torque is also visible in this figure, this is due to the required work to move the finger being constant.

2.6.2 Force analysis

As with the crank, a torque (τ_{center}) can be assumed on the central axis and the force needed on the finger can be derived in the direction of motion. This should again be inversely proportional to the torque analysis of the cam system.

The force in the angular direction at the point of contact is:

$$F_x(\alpha) = \frac{\tau_{center}}{f_{profile}(\alpha)} \tag{2.18}$$

This force is transferred to the bearing under the angle of contact, the transferred force is therefore:

$$F_{cam}(\alpha) = \frac{\tau_{center}}{f_{profile}(\alpha) \cdot sin(\theta_{profile}(\alpha))} \tag{2.19}$$

This force can be split using the same angle into the force parallel to the direction of motion and simplified using the $\frac{cos()}{sin()}$ term:

$$F_{par}(\alpha) = \tau_{center} \cdot \frac{r}{f_{profile}(\alpha)} \cdot (\frac{df_{profile}}{d\alpha})^{-1} \tag{2.20}$$

The forces needed in the direction of movement are plotted in figure 2.15. For these figures a torque of 1 Nm is used. It can be seen that the required forces in the direction of motion in the sine configuration tend towards infinity as the profile reaches the extreme value. This confirms that this relation is again inversely proportional to the previous relation due to a constant required work.

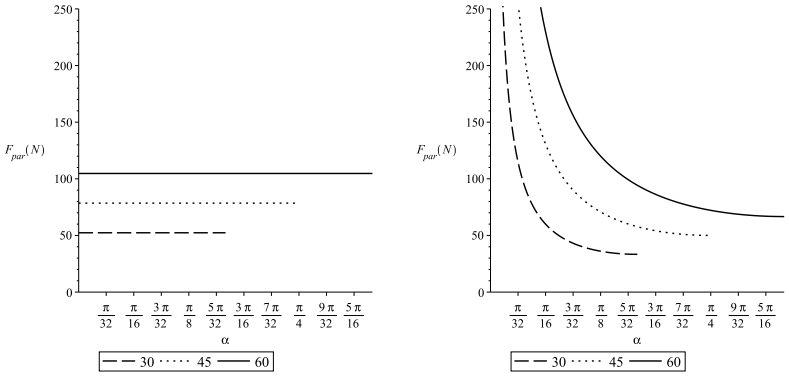

(a) Linear profile *(b) Sine profile*

Figure 2.15: The force in the direction of motion with an input torque of 1 Nm.

Return mechanism

A disadvantage of the cam system is that the cam only pushes the fingers outwards, therefore a system is needed to return the fingers to the opened position. For this system, two possibilities are considered.

Springs

This system relies on springs to pull back the assembly after gripping. The springs have to be able to overcome the friction of the sliding mechanism. This will however induce an extra load of about $5 to 10\,N$, depending on the final assembly, in the closing of the gripper.

Rail system

This relies on the cam to have a similar edge on the other side of the bearing, in this configuration the motor itself has to apply the force to return the assembly to the open position. The downside of this method is the inevitable play in the system as the groove has to be slightly larger than the bearing used.

Conclusion

The disadvantage of the rail system is the extra size of the cam and the extra weight of the assembly. It also introduces some play into the system because the bearing should not touch both sides of the rail at the same time.

The advantage of the spring system over the rail system is that the springs will create a stable position in the opened position. It also helps to keep the fingers in the closed position, as the pull of the springs introduces a small friction between the fingers and the cam.

Due to these two reasons, the spring system is chosen for the final assembly.

2.7 Conclusion

Comparing the crank and cam designs, it can be seen that the construction of a cam system is easier in comparison to the crank, which has 6 joints with 3 links which need to be connected to the finger and the center arm. The cam, attached to the motor shaft, only has contact points with the bearings.

The forces in both the cam and crank designs are comparable for similar displacement angles. Because of these reasons, the cam design is chosen. This design and in particular the cam profile will be refined below.

To compare these profiles, the torque needed to actuate the system is very important, as this is the main constraint in the motor choice. A lower overall torque is beneficial to the forces in the assembly and therefore the material requirements. The final cam will therefore be based on a cam profile with a rotation of 60°.

From the two cam profiles considered, the best fit is the sine profile. Most forces will be applied as the finger contacts the ring, which will be close to the end of the movement, the sine profile causes the the needed torque to decrease when contact is made.

2.8 Size specification

As decided in the previous section, a cam will be used with a sine profile spread over 60°. In this chapter, the actual values for the extreme points will be determined and the analysis will be done again to find the torque needed and forces involved.

Based on the size of the ring and the fingers, a point has been selected on the base of the fingers that moves from $27\,mm$ to $40\,mm$ between opened and closed. With a bearing which has a diameter of $6\,mm$, the surface of the cam needs to vary between $24\,mm$ and $37\,mm$. This size is overall larger than the comparison size earlier in the chapter, this increased size will be beneficial to the cam as it will further decrease the needed torque.

The surface of the cam will be given by the curve in figure 2.16

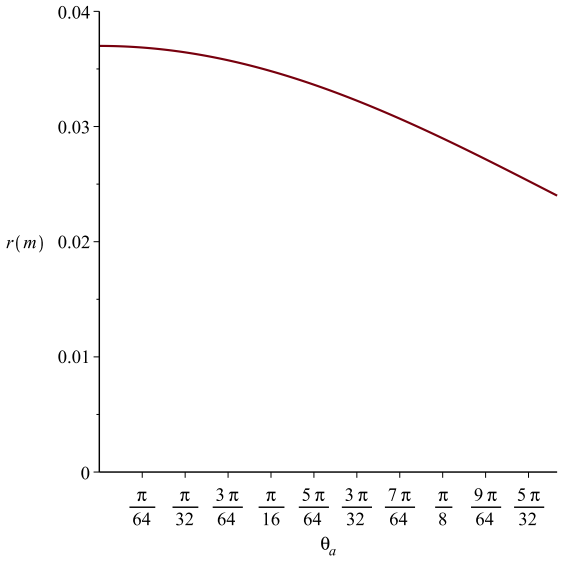

Figure 2.16: The surface of the cam used in the gripper.

To get a feeling for the forces that can be held, figure 2.17 shows the force generated with an input torque of 1 Nm.

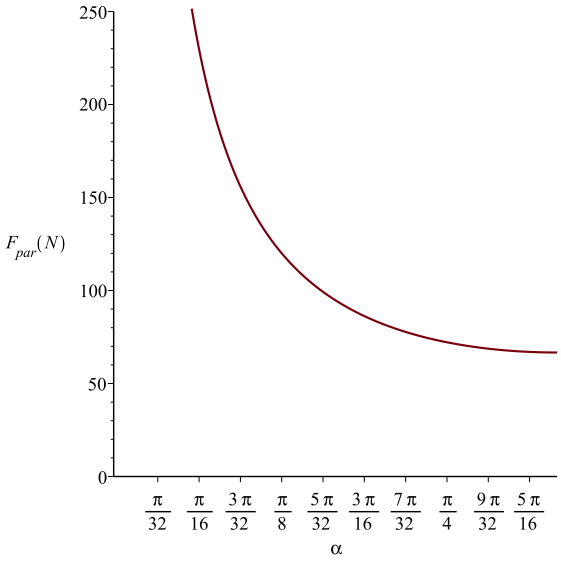

Figure 2.17: The force parallel to the direction of motion that can be held with an input torque of 1 Nm.

Finally, to get a benchmark for the torque needed by the motor, the

induced torque with a load of 45 N is plotted in figure 2.18, this load is composed of 35 N for the weight of the UAV and 10 N for the springs of the return mechanism.

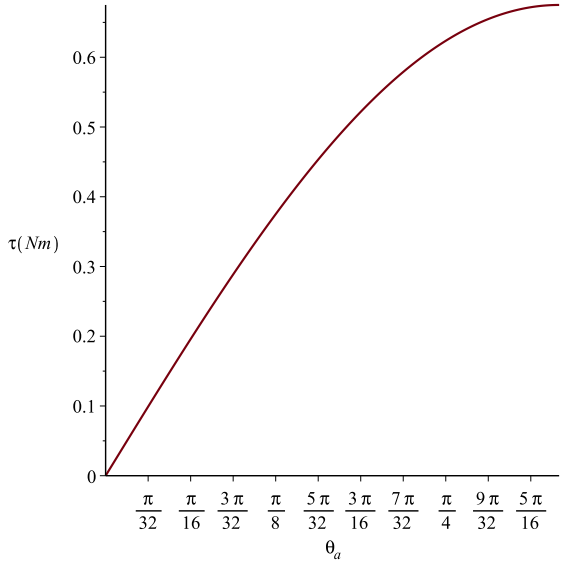

Figure 2.18: The torque needed to hold a load of 45 N.

Chapter 3

Realization

3.1 Introduction

In this chapter a detailed description of all the parts that make up the assembly will be given.

3.2 Assembly

The contact point of the finger assembly with the cam will be a bearing with a diameter of $6mm$, this bearing will be attached using a custom pin with a diameter of $3mm$ which will extend past the bearing and the cam to provide a space in which to attach the springs.

A cross-section view of the assembly can be seen in figure 3.1, it can be seen in more detail in Appendix A.

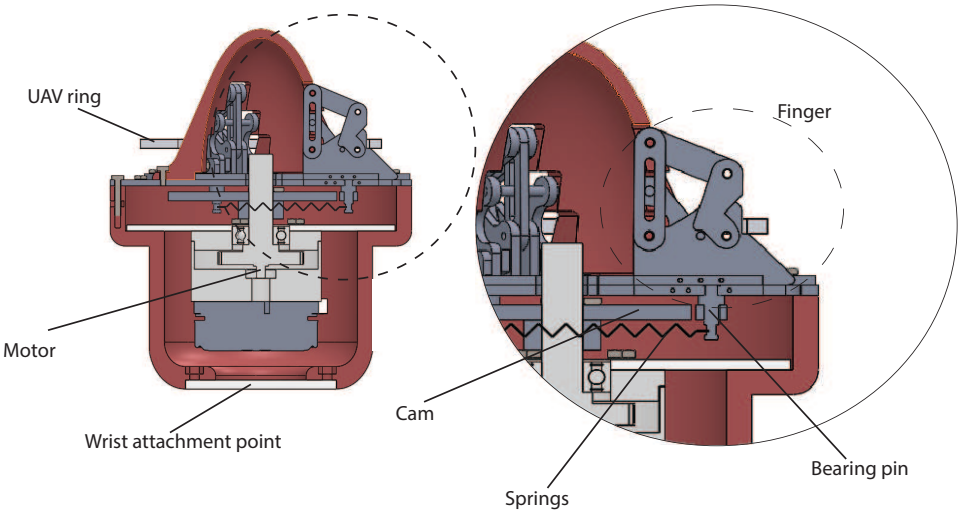

Figure 3.1: Cross section view of the assembly.

3.3 Guiding point

To guide the gripper towards the interface on the UAV, a point has been mounted on top of the gripper. Additionaly, this point also provides a cover for the fingers to keep out dust and other contaminants and protect them against accidental contact. The point and how it is mounted can be seen in figure 3.2. This point will increase the error margin by about $20 - 25\,mm$.

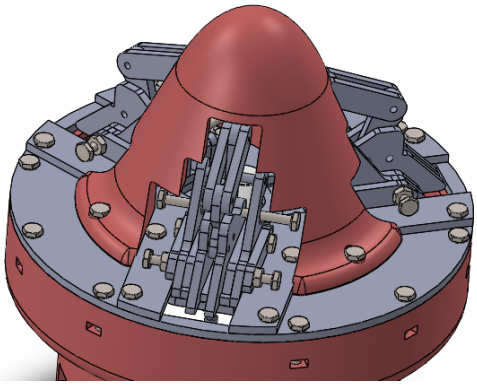

Figure 3.2: The guiding point as it is mounted on the gripper.

3.4 Fingers

The fingers are the contact points between the assembly and the UAV, they consist of multiple small parts each. The fingers will be actuated using a rotating cam. Contact will be made using a bearing that is secured on a custom made pin that extrudes from the bottom of the finger assembly. This pin will also feature a cut-out to attach the springs to retract the fingers in the closing motion.

Figure 3.3 shows a simplified drawing of how the cam and springs are in contact with the finger, it is important to note that the springs are attached to the peg and the cam is in contact with a bearing on the peg.

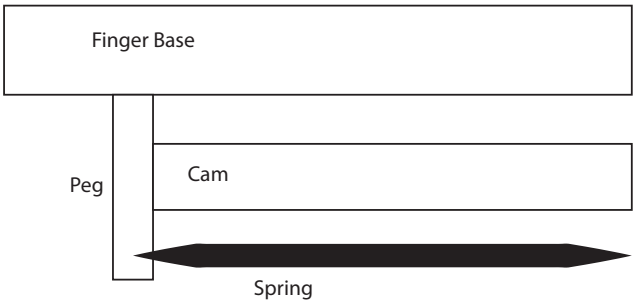

Figure 3.3: Overview of the elements in contact with the finger peg.

The parts of the fingers will be lasercut from Delrin and assembled using bolts.

An exploded view of one the fingers can be found in figure 3.4.

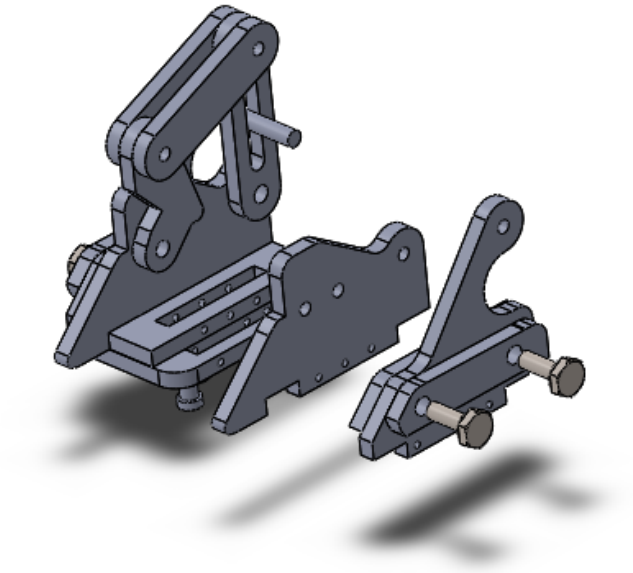

Figure 3.4: Exploded view of the finger.

3.5 Cam

As concluded in the previous chapter, the design will be using a cam with a sine profile and an angular displacement of 60° between high and low points. This design will be symmetrical around the center to create a constant surface.

In its most simple form, it would be half a sine wave, as seen in figure 3.5.

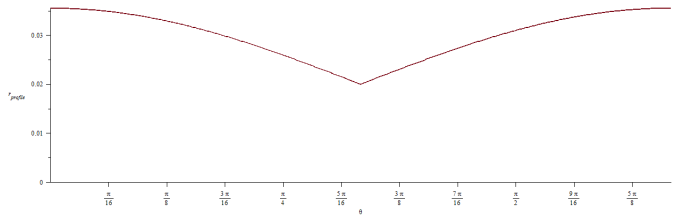

Figure 3.5: The profile as half a sine wave.

However, this design lacks a smooth transition in the open position. To solve this, a partial parabola will be added between the waves as visible in figure 3.6.

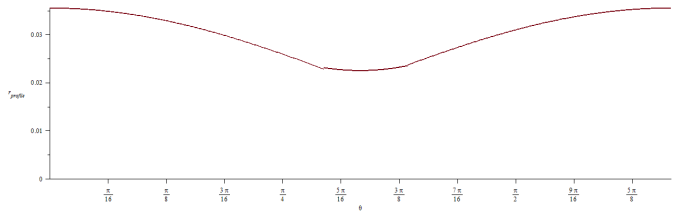

Figure 3.6: The profile with a parabola added between the waves.

After this it was found that the top of the sine was not level enough to ensure a fixed position. To overcome this, the sine wave was limited to 53° and a flat plane of 7° was added in between. This final profile is visible in figure 3.7.

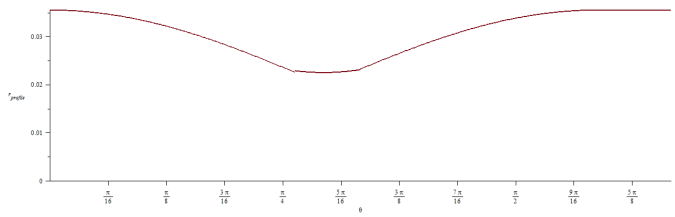

Figure 3.7: The profile with a flat area added.

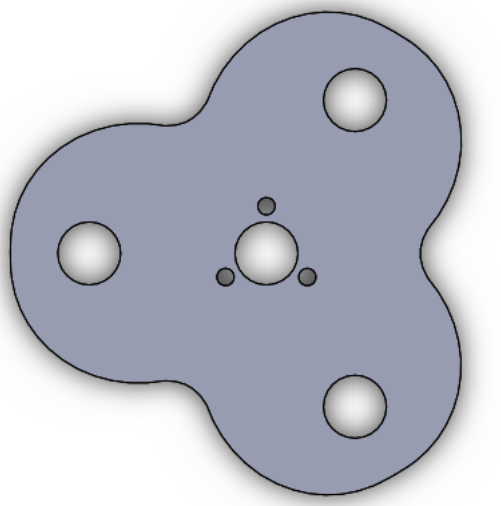

Figure 3.8: The final cam as implemented in the system.

The cam surface will be lasercut and a seperate ring will be used to attach it to the motor shaft

3.6 Springs

The springs are used as a return mechanism and the force of them should be high enough to overcome the friction of the sliding mechanism. To overcome the friction in the system and to ensure opening of the gripper, the springs should provide a force between roughly $5N$ and $10N$. These springs will be attached to pins in a triangle configuration, this means that all pins will be connected to each other but not to the housing itself. This can be seen in Figure 3.9, where only the springs are visible, the cam will be mounted between the pegs.

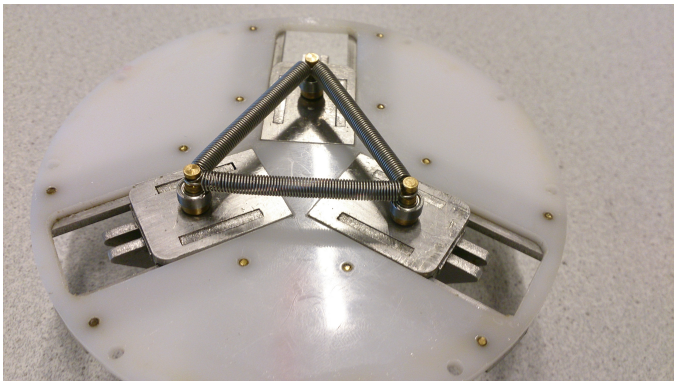

Figure 3.9: The realization of the springs in the final assembly.

3.7 Actuation

For the actuation of the gripper, as suitable motor has to be found. From figure 2.14 it can be found that for the 60° sine profile, the motor should be able to generate at least 0.7 Nm to move the gripper. In addition to this torque requirement, the motor should have sufficient power to drive the actuation at an acceptable speed.

The second most important aspect of the motor is the size it takes up in the assembly, as the gripper should be as short as possible.

The motor will be made using a combination of maxon parts, 2 different modules (motor + gearbox) will be combined to choose the final motor [2]. Four combinations [1] have been selected from the maxon catalog with criteria relating to the previously stated requirements. They have all been chosen from the EC flat range, which are currently the smallest brushless motors in the catalog.

[1]Maxon part numbers (motor + gearbox):
1: 200142 + 266595
2: 200142 + 301171
3: 339282 + 301173
4: 402687 + 301185

Combination	1	2	3	4
Output Torque (Nm)	1.76	2.585	1.716	21.842
Cost (€)	208.45	208.45	216.81	259.46
Length (mm)	39.9	39.9	39.9	53.6
Weight(g)	295	295	295	390
Reduction ratio	32:1	47:1	26:1	163:1
Power(W)	30	30	30	70
Nominal output speed (rpm)	91	62	127	16

Table 3.1: Motor specifications of the four combinations.

From table 3.1, where 4 possible motors are compared, it can be seen that combination 4 produces too much torque and is too heavy. From the remaining three options, combination 2 is the best fit, as it has the highest output torque and the speed is enough to theoretically close the gripper in 0.3 *sec*. This motor will be used in the final assembly.

3.8 Electronics

The gripper will be powered by means of an Elmo motor controller [1]. This Elmo will be mounted on the lower arm, as space is scarce on higher parts of the arm (wrist + gripper). A breakout board will be mounted inside the gripper to allow regular cables to be routed to the controller.

Additionally, the motor needs a sensor to find out the position of the motor and relay it to the controller. The motor will has built-in hall effect sensors, which combined with the gearbox will give sufficient resolution.

These sensors will only measure a relative position, it is therefore unknown in which state the system is as the system starts. A calibration system is needed and will be described in the following section.

3.9 Calibration

Calibrating the gripper will use the fact that in rotating, there are two stable positions(open and closed) and an unstable area in between, these areas are visualized in figure 3.10. When first starting the gripper, it can be assumed that the gripper is in either of these stable positions. It will therefore turn to the unstable area between open and closed and then fall back into the open stable position.

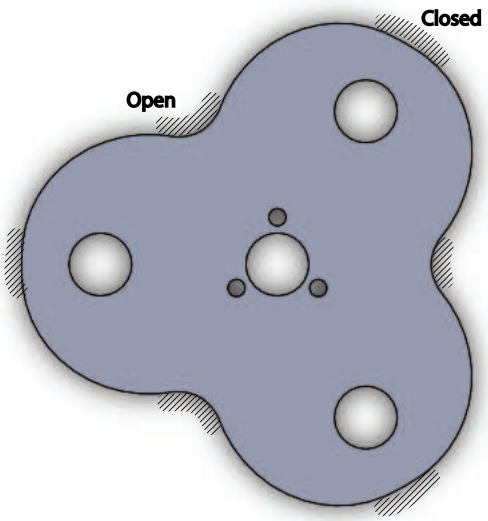

Figure 3.10: Indication of stable (hatched) and unstable (unhatched) positions on the cam.

The software for the gripper will be written in ROS (Robot Operating System) [3] in an environment prepared by Willem Boterenbrood [4]. The code written is for the calibration of the gripper, which takes the following algorithm:

1. Turn 188 counts to an unstable position
2. Release motor to fall back to the opened stable position

This can be realized by creating two states in the software, the first will tell the motor to turn 188 counts and then waits for the Elmo to respond that it has indeed turned to 188 counts. This triggers a transfer to the second state in which the motor is turned off, causing the motor to freewheel into it's open stable position. The code that handles this behavior can be seen found in appendix B.

Chapter 4

Testing

4.1 Closing speed

An important aspect of the gripper is the time it takes to go from receiving a closing command to being fully closed.

After trying several speeds it was found that the gripper could reliably close at its fastest speed of 3000 rpm (this is the target speed of the motor, the output target speed is 47 times less), this however had the same closing time as a target speed of 2500 rpm. The graph in figure 4.1 shows the position of the gripper plotted against time for three considered cases. This shows that after about 0.2 *sec*, the target position was reached and after about 0.5 *sec* the system was at rest again in the case of 2500 rpm. This speed is of course without any resistance from the UAV, only the movement of the fingers and the resistance from the springs are acting on the motor, nevertheless this speed is in line with the requirements.

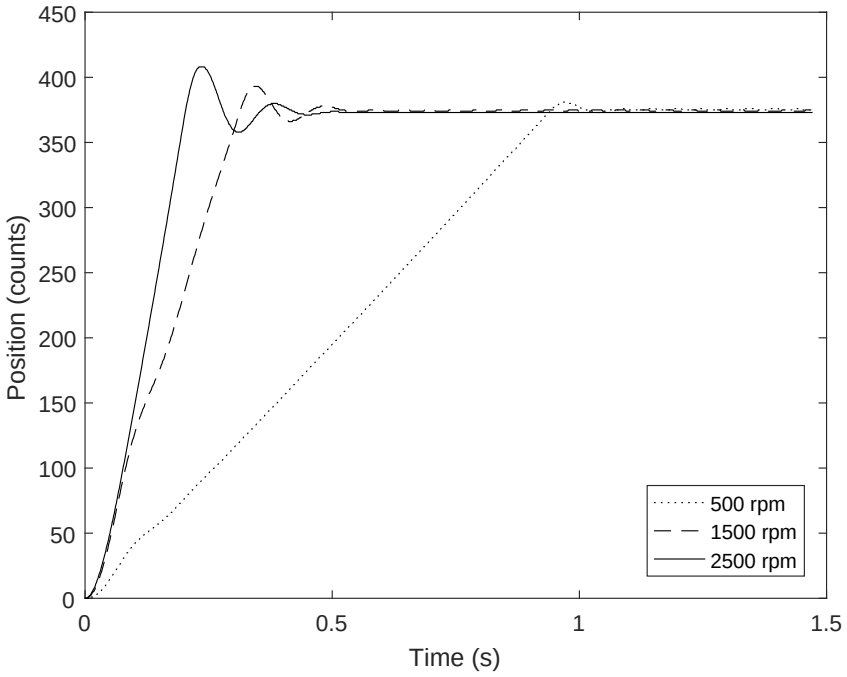

Figure 4.1: Position of the gripper during closing procedure for three different target speeds.

4.2 Strength

To test the strength of the gripper, a dummy weight of 2.5 kg has been attached to the gripper. It was able to hold this weight in various orientations.

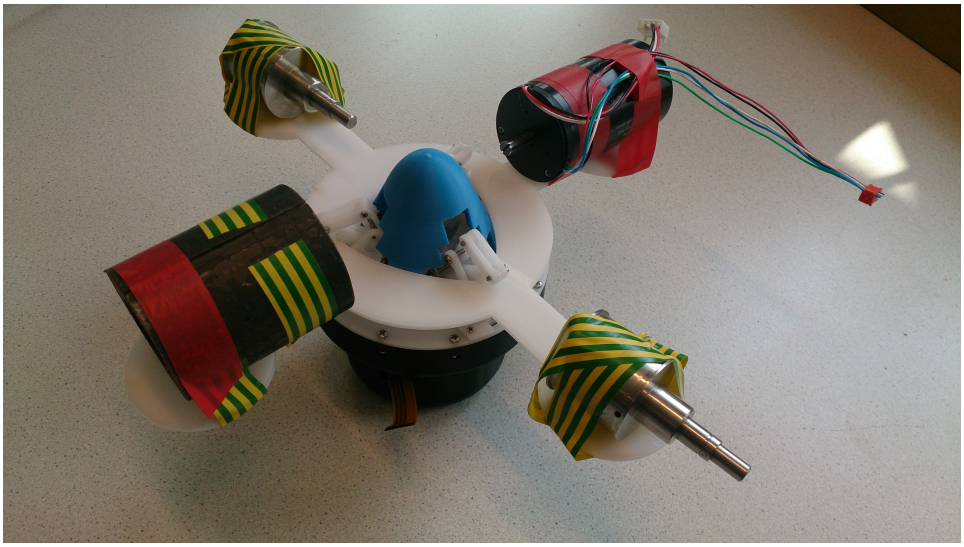

Figure 4.2: The dummy weight attached to the gripper.

4.3 Conclusion

According to the tests of closing speed and strength, the requirements set in the introduction have been met. Closing speed is 0.5 sec, the same as the requirement. The gripper was also able to hold the expected payload of 2.5 kg.

Chapter 5

Conclusion

For the actuation mechanism, a choice was made between three different options: A system based on an inner gear with a radius which was half of the radius of the outer gear, a crank-based system which moves the fingers using jointed arms and a cam-based system with a central cam against which the fingers rest.

At first, the half-gear design was discarded due to the impracticality of needing three separate gears overlapping in a tight space.

After comparison of the two remaining concepts, it was clear that the cam system was superior over the crank system. The cam system had more effective force and it was structurally easier to realize

An analysis has also been applied to the fingers to see if there is a better orientation with respect to the old design. It became clear that increasing the length of the back linkage increased the closing angle while also creating a sloped upper surface to help guide the gripper into the interface. This guiding effect is also introduced by the point fitted on top of the gripper.

Calibration of the gripper will be done using the stable point in the cam rotation, which are at the fully opened and fully closed points of the gripper. By rotating the cam between two stable points and shutting off the motor, the system will automatically fall back into the fully opened stable position.

5.1 Learning points

After construction of the first prototype gripper, some points were found for improvement:

- The friction in the fingers is too high due to the friction of steel on steel, this has been solved by using Delrin to create the fingers
- The fingers were susceptible to dust and other outside influences, this has been improved by adding a housing for the fingers.
- It is hard to aim the gripper due to a margin of about 1 cm, this has be solved by creating a cone-shaped structure on top of the gripper to guide it into place.
- The gripping interface was not rotationally locked, this has be solved by using a different shape as interface which automatically rotates to the desired rotation as the gripper closes.

5.2 Recommendations for future work

For future work, it is recommended to re-evaluate the design of the finger. It is hard to manufacture in its current form and still quite delicate.

Appendix A

Assembly

In this appendix, the assembly of the fingers and the actuation mechanism will be shown and a detailed assembly instruction is given.

A.1 Finger

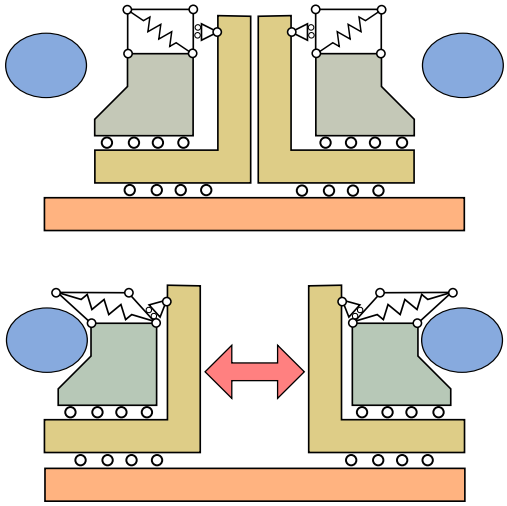

Figure A.1: Conceptual drawing of the finger.

In figure A.2, the total assembly of the finger can be seen, including the two attachment points for springs, which are the bolt on the front of the base and the extruding pin on the moving part.

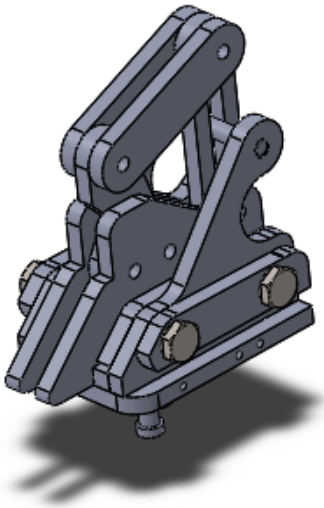

Figure A.2: Overview of the finger.

A more detailed look on the inner workings can be seen in figure A.3

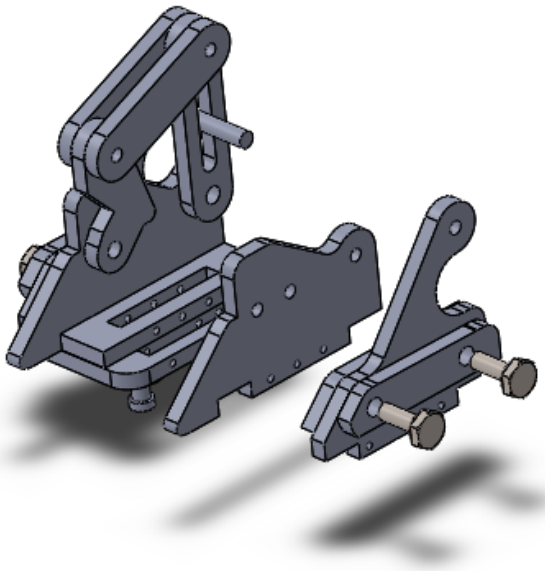

Figure A.3: Exploded view of the finger.

A.2 Finger attachment

To attach the fingers to the gripper, two plates are used as sliding guides for the fingers, as can be seen in figure A.4

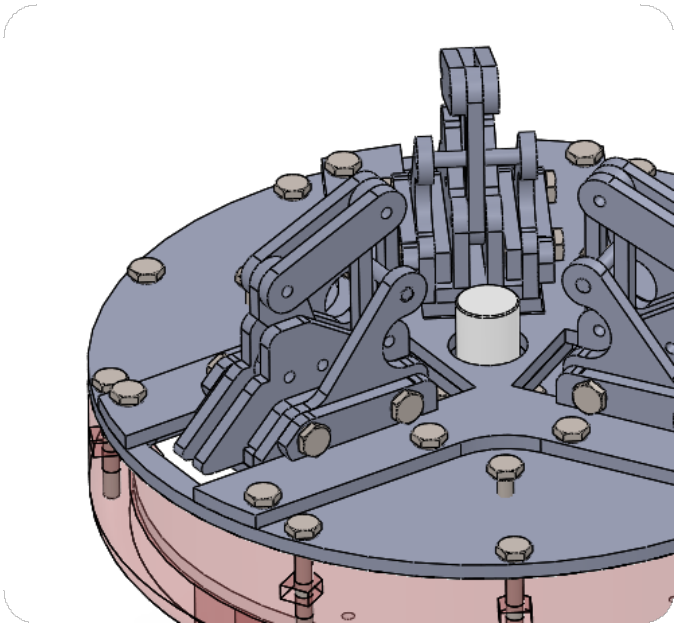

Figure A.4: Overview of the attachment of the finger to a base plate.

A.3 Actuation

To actuate the fingers, they will be equipped with a specially designed bearing peg that will hold a bearing to contact the cam. It also features a cut-out to hold springs for the retraction mechanism. The peg itself can be seen in figure A.5, the top part (above the flange) will be threaded to be screwed into the bottom of the finger. The bearing will be located just below the flange and springs will be rested in the cut-out. Figure A.6 show how the peg and the bearing are attached to the finger assembly. These bearings rest against a cam located in the gripper, which is shown in figure A.7.

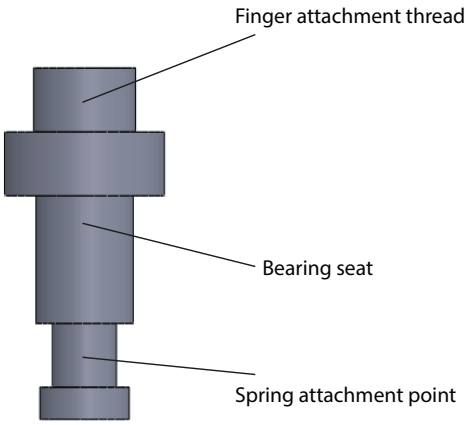

Figure A.5: Detail of the peg itself.

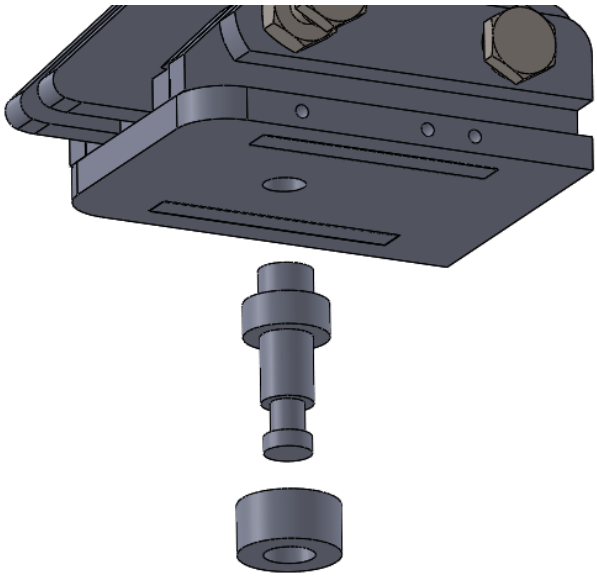

Figure A.6: Overview of the attachment of the bearing to the finger.

A.4 Detailed assembly instructions

In this section a complete and very detailed assembly instruction will be given to create the final product.

1. The first step in assembling is assembling the fingers, they are held together using M2 bolts that screw into the plastic. The side plates can be fixed in the base using glue or a rod inserted through the side. The hole in the bottom of the finger should be tapped to M3 to accommodate the bearing pin.
2. The bolts in the front of the outer assembly and in the lower back of the inner assembly should extend out about $2\,mm$ to allow the springs to be fitted.
3. The bearings should be pressed onto the bearing pins until they fit against the wide band.
4. These pins can then be screwed into the M3 holes in the bottom of the finger assembly.
5. Using the guide and the base, three finger assemblies can be combined into the top part of the gripper. The printed point can be attached on top of this assembly.
6. Seperately, the motor can be attached to its baseplate and the cam with the ring can be attached to the motor. The distance between the bottom of the cam and the top of the baseplate should be $8\,mm$.
7. If this is done correctly, there should be about $12\,mm$ of motor shaft above the surface of the cam. This excess can be put in the hole in the middle of the finger assembly, by lining up the cam with the bearings on the pin, there should be room for the springs to be attached.
8. The bearing pins can be joined together by arranging three springs between them. The springs should be in a triangle configuration if it has been done well.
9. This whole assembly can then be lowered into the gripper housing and can be fixed in place using bolts.

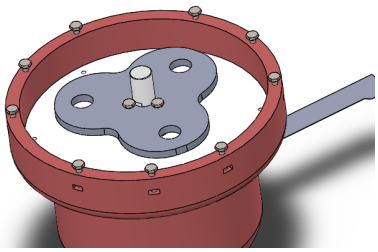

Figure A.7: Location of the cam in the assembly.

Appendix B

Code

This is the code used to calibrate the gripper. It first rotates the motor 188 counts and then turns it off, allowing it to freewheel into a known position. It has been written in ROS [3] using a framework prepared by Willem Boterenbrood for the SHERPA project [4]

```
void St_Calibration_Gripper::entry()
{
        ROS_INFO("State Change: Gripper Calibration [%s - %d]",
             machine_ptr->RCIstruct_ptr->ifname.c_str(),
            machine_ptr->node_id);
        machine_ptr->goto_position(188);
        machine_ptr->start_movement();
}

void St_Calibration_Gripper::dataFromCAN(struct can_frame2
    frame2)
{
        if (frame2.data[0] == EC_P && frame2.data[1] == EC_X )
             // Position data from Elmo
        {
                int pos = machine_ptr->getPosition(frame2);
                position_data_handler(pos);
        }
}

void St_Calibration_Gripper::position_data_handler(int pos)
{
        if (pos > 186 && pos < 190)
        {
                machine_ptr->stateChange<
                    St_Calibration_Gripper_2>();
        }
}

void St_Calibration_Gripper_2::entry()
{
```

```
        ROS_INFO("State Change: Gripper Calibration 2 [%s - %d]
            ", machine_ptr->RCIstruct_ptr->ifname.c_str(),
            machine_ptr->node_id);
        machine_ptr->set_motor_off();
        ROS_INFO("done");
        sleep(5);
        setCalibratedParam();
        machine_ptr->stateChange<St_Operation>();
}

void St_Calibration_Gripper_2::setCalibratedParam()
{
        std::string param_name = ros_params::NODES;
        std::string array_name = ros_params::
            NODES_ELMO_CALIBRATION_DONE;
        try{ros_params::setArrayParameterN(param_name,
            array_name, machine_ptr->array_position, 1);} //
            Set the calibration done bool for this joint in the
             ROS parameter server for other nodes to check
        catch (int){ROS_ERROR("Unable to set position %u in
            parameter %s of array %s, in the ROS params",
            machine_ptr->array_position, param_name.c_str(),
            array_name.c_str());}
```

Bibliography

[1] Elmo motor controller. Online, accessed April 2016.

[2] Maxon motor. Online, accessed April 2016.

[3] Ros: Robot operating system. Online, accessed April 2016.

[4] Willem Boterenbrood. Development of the low-level software architecture for the sherpa robot arm. *University of Twente*, 2015.

[5] M. Braccio, D.W. Gross, J.J. Zimmer, and J.R. Badura. Special purpose robotic end effector, 1990. US Patent 4,905,938.

[6] L. Marconi et al. The sherpa project: smart collaboration between humans and ground-aerial robots for improving rescuing activities in alpine environments. *IEEE International Symposium on Safety, Security, and Rescue Robotics (SSRR)*, 2012.